The 2013 World Congress on
Advances in Structural Engineering and Mechanics (ASEM13)
Jeju, Korea, September 8-12, 2013

FEA modelling of curved concrete filled steel tubular (CCFST) trusses subjected to bending

*Wu Xu[1)], Lin-Hai Han[2)] and Zhong Tao[3)]

[1), 2)] *Department of Civil Engineering, Tsinghua University, Beijing, 100084, China*
[3)] *Institute for Infrastructure Engineering, University of Western Sydney, Penrith, NSW 2751, Australia*
[1)] xuwu11@mails.tsinghua.edu.cn

ABSTRACT

The curved concrete filled steel tubular (CCFST) truss is a new type of truss with curved CFST chords and hollow braces. A finite element analysis (FEA) model of the CCFST truss subjected to bending was developed. The FEA model was verified by a series of tests conducted before. Good agreement was obtained between the numerical results and the experimental results in terms of failure modes, load versus deflection curves and strain development. It was found that a typical load versus deflection curve can be divided into three stages: elastic stage, yielding stage and hardening stage. The FEA model was further used to investigate the stress and strain developments of the structure by full range analysis.

Keywords: Concrete filled steel tube (CFST), Curved truss, Finite element analysis (FEA), Full range analysis.

1. Introduction

The curved concrete filled steel tubular (CCFST) truss is a type of truss curved in shape and has tubular chords filled with concrete. Compared with the truss with hollow tubular chords, buckling behaviour both in and out of the loading plane could be improved because the concrete filled steel tubular (CFST) chords can provide larger flexural stiffness. Local buckling of the chord, especially around the joint, can be prevented or delayed due to the support from the core concrete to the steel tube. Thus the strength and ductility of the whole structure are improved. Also, the infill concrete could increase the fire resistance of the structure. Owing to the above benefits, CCFST trusses have been the interests of more and more structural engineers.

It is well known that CFST members have an excellent performance in compression with high strength and good ductility. Meanwhile the trusses have been widely used due to the effective force transferring mechanism. At present, a large

[1)] Graduate Student
[2)] Professor
[3)] A/Professor

number of studies have been conducted on CFST members (Han 2004 & 2011, Varma 2002, Tao 2011, Lu 2009) and steel tubular trusses (Rahami 2008, Jin 2011). Kawano (2000 & 2003) studied the deformation capacity of 2-chord CFST trusses under monotonic and cyclic loading. Fong (2011) conducted tests of two trusses composed of CFST members and hollow tubular members to investigate the buckling behaviour of CFST trusses. Han (2012) reported a series of tests on 3-chord CCFST members subjected to axial compression. However, till now, the behaviour of CCFST trusses under bending or combined bending and shear has seldom been reported yet.

In the paper, a finite element analysis (FEA) model of the CCFST truss subjected to bending was established. The accuracy of the FEA model was verified by a series of tests conducted by the research group earlier, including 4 CCFST trusses, 2 straight CFST trusses and 2 hollow tubular trusses. Based on the FEA model, a full range analysis was conducted, which provided a comprehensive understanding of the flexural behaviour of the structure.

2. Finite element analysis (FEA) model

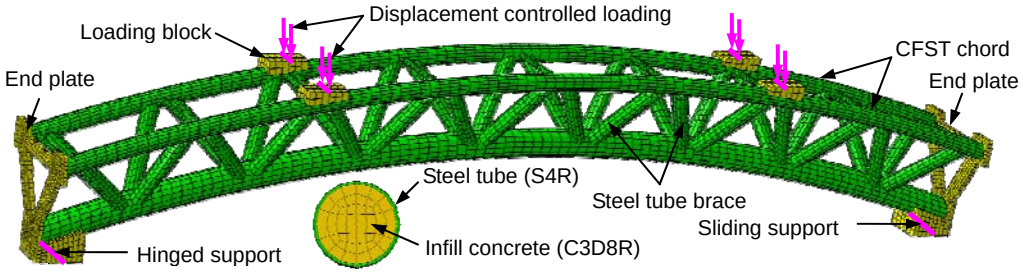

Fig. 1 Finite element analysis model for the CCFST truss

To further analyse the flexural behaviour and force transfer mechanism of CCFST trusses, a finite element analysis (FEA) model was established based on the commercial FEA package, ABAQUS (2004). Fig. 1 gives a schematic view of the FEM model of the CCFST truss. The curved chord is generated through the sweep of a circular section, while the braces are obtained by the cut operation provided by the software. The chords and braces are assembled together according to their spatial location. In order to avoid stress concentration, loading blocks are used to transmit the vertical load. Simplification of the boundary condition is applied at two ends of the truss, where the specimen is simply supported. As shown in the figure, the truss is loaded by four point loading method. To achieve a good convergence performance, displacement controlled loading method is utilised.

Four-node shell elements with reduced integration (S4R) are used for the steel tube, whilst the 8-node linear brick elements with reduced integration (C3D8R) are applied for the infill concrete, end plates and loading blocks. A proper mesh size is chosen to achieve a balance between the convergence and the computing time.

The FEA model takes both the geometric nonlinearity and material nonlinearity

into consideration. The former is controlled by the software which allows the model to include the effect of large deformation, while the latter is realised by the nonlinear material property of the concrete and steel. Details of the material model of infill concrete can be found in Han (2007), where plastic damage model provided by the software was used for the concrete and a modified uniaxial stress versus strain curve of confined concrete was proposed. For the carbon steel in the test, an elastic–plastic stress versus strain model composed of five stages can be adopted. However, in order to verify the model, the measured stress versus strain curves of steel is used.

Interaction is another important factor to be considered in the FEA model. “Hard contact” is applied for the surface interaction between the concrete and steel tube with a friction coefficient of 0.6 which is recommended by Han (2007). In terms of the interaction between the chords and braces, the “tie” constraint is defined for them.

3. Verification of the FEA model

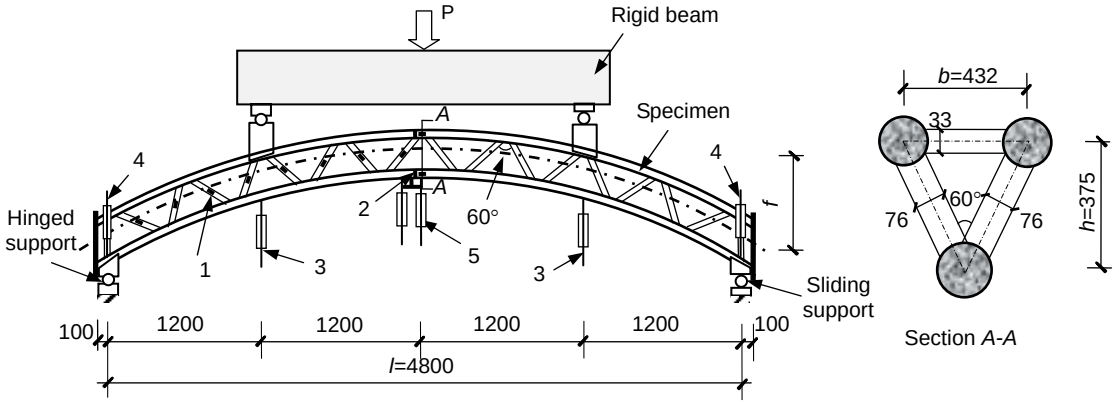

1. Strain gauge of brace
2. Strain gauge of chord
3. Displacement transducer to measure vertical deflections
4. Displacement transducer to measure support settlements
5. Displacement transducer to measure curvature

Fig. 2 Test set-up and specimen configuration (Unit: mm)

A series of tests conducted by the research group is used to verify the above FEA model. The test set-up and details of the CCFST specimens are shown in Fig. 1, where P is the vertical load applied on the specimen; f and l are the arch rise and effective span of the truss, respectively. The curved specimen is a circular arc in shape defined by the rise-to-span ratio (f/l). The main parameters considered were the rise-to-span ratio (f/l) and type of chords. Detailed dimensions of all the specimens are given in Table 1, where specimen designations starting with T and TH represent trusses with CFST chords and steel tube chords, respectively. Duplicate specimens were prepared to guarantee the reliability of test results. The loading and measuring devices of the test set-up are also shown in Fig. 1. The measured overall diameter (d), thickness (t), yield strength (f_y), tensile strength (f_u), elastic modulus (E_s) and Poisson’s ratio (μ_s) of the steel tubes are shown in Table 2. At the time of tests, the measured average cubic compression strength of infill concrete was 69.9 N/mm^2 and the elastic modulus was 36400 N/mm^2.

Table 1 Summary of specimen information

No.	Specimen labels	Rise-to-span ratio *f*/*l*	Chord type	Failure mode	P_u (kN)	$P_{u,FEA}$ (kN)	P_{max} (kN)
1	T1-1	0	CFST	Bending	341	391	450
2	T1-2	0			341		452
3	T2-1	0.1	CFST	Bending—shear	471	446	556
4	T2-2	0.1			476		524
5	T3-1	0.2			460	457	525
6	T3-2	0.2			483		503
7	TH4-1	0.1	Steel tube	Local buckling	--		310
8	TH4-2	0.1			--		318

Table 2 Summary of steel properties

Steel type	*d* (mm)	*t* (mm)	f_y (N/mm^2)	f_u (N/mm^2)	E_s (N/mm^2)	μ_s
Bottom chord	140.02	3.94	320	454	2.14×10^5	0.283
Top chord	88.12	2.95	323	445	1.92×10^5	0.289
Diagonal	75.92	3.00	338	446	2.15×10^5	0.294
Transverse	33.00	2.69	368	461	2.02×10^5	0.302

The typical failure modes of the straight CFST truss, CCFST truss and hollow tubular truss are shown in Fig. 3. Fig. 3(a) shows the failure mode of the CFST trusses which can be characterised as bending failure. No local buckling or weld fracture was observed during the loading process and the test stopped when the displacement at mid-span reached *l*/40. Fig. 3(b) shows the failure mode of CCFST trusses which can be characterised as bending-shear failure. At the early stage of loading, the steel tube of the bottom chord yielded first, but the load kept increasing. Upon further loading, weld fracture occurred at either one of the top or bottom chord joints located within the shear span. The load then dropped suddenly because of the fracture located within the weld or immediately adjacent to the weld in the heat-affected zone. Fig. 3(c) shows the failure mode of hollow tubular trusses which is local buckling failure. The local buckling occurred at the top chord joint within the shear span of the truss subjected to combined bending and shear.

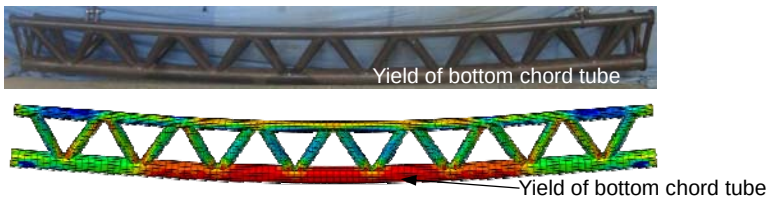

(a) CFST truss (Bending failure)

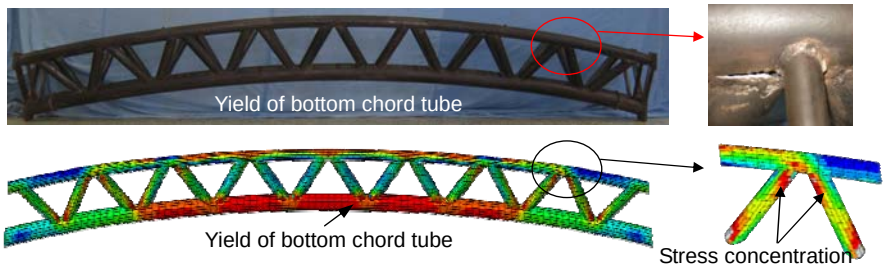

(b) CCFST truss (Bending-shear failure)

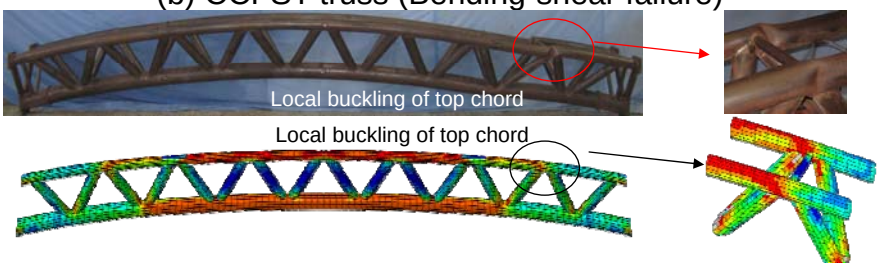

(c) Hollow tubular truss (Local buckling failure)

Fig. 3 Typical failure modes of specimens

The predicted results of failure modes are also shown and compared with the experimental results in Fig. 3. Distribution of the Mises stress is also shown. It can be seen that the predicted results achieve a good agreement with the experimental results in specimen deformation. Despite the fact that the current FEA model is not able to simulate the local failure accurately, the stress distribution explains the local failure of the joints.

The measured load (P) versus mid-span deflection (u_m) curves for all the tested specimens are shown in Fig. 4. For CFST trusses, they demonstrated excellent ductility during the loading process, as shown in Fig. 4(a). But for all the CCFST trusses, there was a sudden drop in strength when the peak load was achieved as shown in Fig. 4(b) and Fig. 4(c). This is because of the joint failure as described before. However, after the joint failure, the shear force was bear by the adjacent braces and the load increased again due to the force redistribution until reaching a second peak load which was lower than the former. Compared with trusses with CFST chords, the load-carrying capacity and deformation capacity of the hollow tubular truss is low, as shown in Fig 4(d).

The predicted P versus u_m curves are also shown and compared with the measured results in Fig. 4. It can be seen that in the initial stage of loading, there is a good agreement between the two, whilst some difference occurs after the stiffness degradation. Generally, the FEA model can reasonably simulate the P versus u_m curves of the specimens with CFST chords (specimens T1, T2 and T3) before the local failure occurs. As for the hollow tubular trusses (specimens TH4), the predicted results overestimate the load-carrying capacity of the specimens, which may due to the initial imperfections and the welding residual stress which are not considered in the current model.

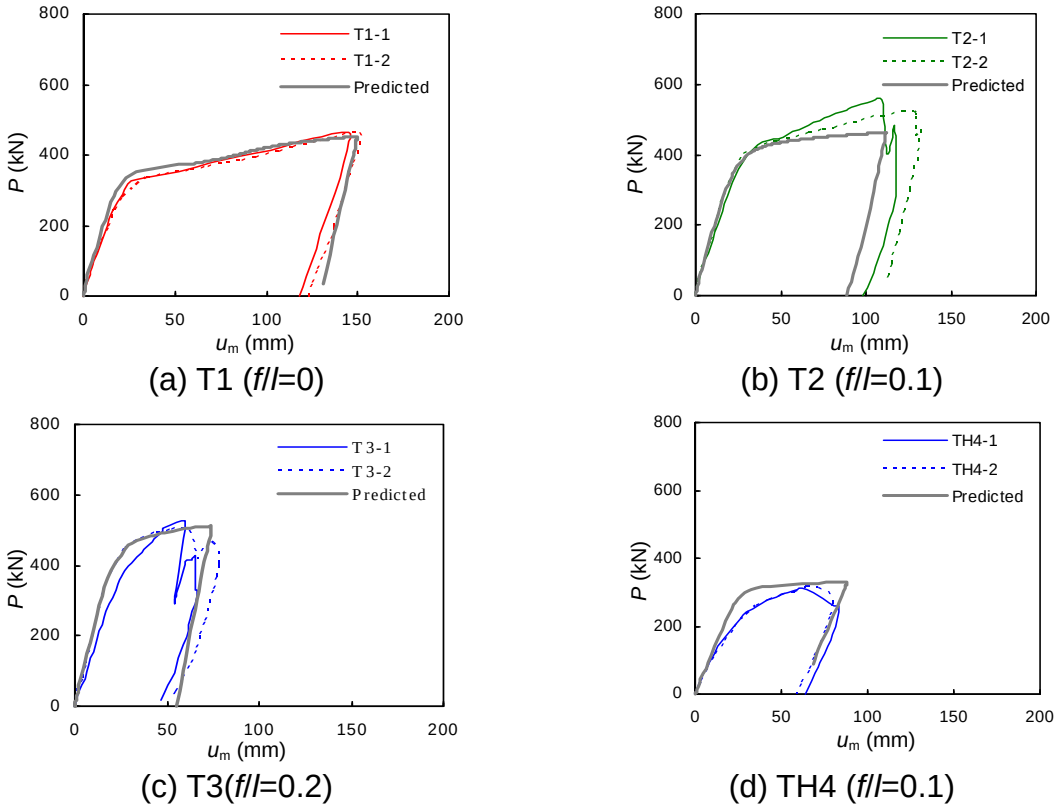

Fig. 4 Comparison of predicted P-u_m curves with measured results

Fig. 5 shows the measured and predicted load (P) versus longitudinal strains (ε) curves of chords at mid-span (T2-1). The negative strain denotes compressive strain of the top chord, whilst the positive strain denotes tensile strain of the bottom chord. Generally, the predicted strain is larger than the measured strain. However, the two sets of curves show the same developing tendency, which can be obtained by the comparison of typical points. The yield strains of the corresponding steel tubes (-1682 $\mu\varepsilon$ and 1495 $\mu\varepsilon$) and the ultimate strain (10000 $\mu\varepsilon$) are indicated by vertical lines in both figures, respectively. Typical points A, B and C corresponding to the yield strain of bottom tube, top tube and ultimate strain of the bottom tube, respectively, are obtained. It can be seen that in both figures, owing to the configuration of the cross-section, strain of the bottom chord is much larger than that of the top chord. Within the parametric limit of the tested specimens, the bottom tube yields before the top tube and the top tube yields before the ultimate strain of the bottom tube is reached.

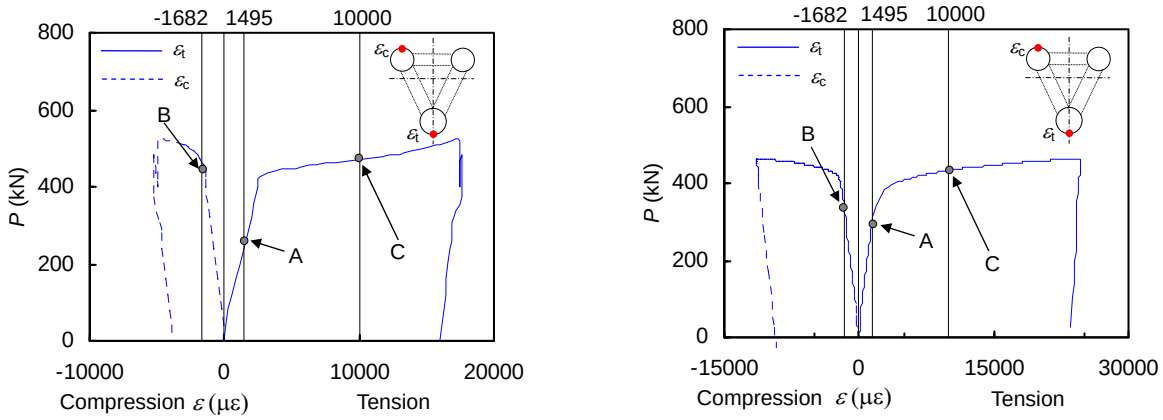

(a) Experimental result (b) Predicted result

Fig. 5 Typical load (P) versus longitudinal strain (ε) curves of chords at mid-span (T2-1)

4. Full range analysis

4.1. Load versus mid-span deflection curves

Generally, for a properly designed CCFST truss, local failure will not happen before the yielding of the bottom chord. Thus the flexural behaviour can be reasonable reflected by the P versus u_m curve without considering the joint failure. Using the FEA model, the predicted P versus u_m curve of a typical CCFST truss T2-1 is used in the following for behaviour analysis. The P versus u_m curve is divided into three stages.

Stage 1: Elastic stage (OA). All the chords and braces work in the elastic phase. The steel tube of the bottom chord yields at point A and the corresponding load is defined as P_{y1}. The concrete in the bottom chord begins to crack. The elastic stiffness K_e of the P versus u_m curve is defined as the secant stiffness when the load reaches $0.2P_u$ where P_u is the ultimate load defines as below.

Stage 2: Yielding stage (AB). During this stage, concrete in the bottom chord has completely cracked, and provides negligible carrying capacity. The load carried by the bottom chord increases slowly since the majority of the steel cross-section at mid-span has yielded. Strain in the steel tube of the top chord continues to increase and reaches the yield strain at point B, resulting in a continuous decrease of the stiffness. The load at point B is defined as P_{y2}.

Stage 3: Hardening stage (BD). During this stage, the load increases slightly but the displacement increases rapidly. Stiffness in this stage keeps almost constant and can be defined as the plastic stiffness (K_p). The longitudinal strain of the bottom chord at mid-span reaches 10000 $\mu\varepsilon$ at point C. According to the method of Han (2004), the load corresponding to point C is defined as the ultimate load (P_u) in this paper, where the capacity of the bottom chord is almost fully utilised. Generally, if the top chord is strong enough, P_u is larger than P_{y2}, which is the case of the tested specimens. At point D, the peak load P_{max} is achieved.

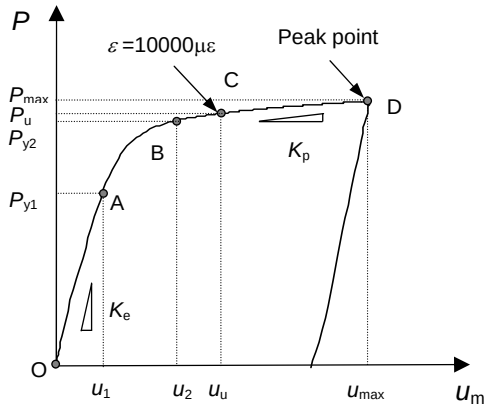

Fig. 6 Typical load (P) versus deflection (u_m) curves (T2-1)

Values of P_u and P_{max} for all the specimens are presented in Table 1. On average, P_u is 83.6% of P_{max}. The predicted ultimate load $P_{u,FEA}$ is also listed in Table 1. The corresponding $P_u/P_{u,FEA}$ ratio ranges from 0.872 to 1.067 and the average ratio equals 0.989.

4.2. Stress and strain development

Generally, the stress and strain increase as the vertical load increases, but this is not always true for all the section. Stress redistribution occurs as the vertical load leads to the plastic deformation in the truss section. Meanwhile, the nonlinearity of the steel and concrete materials will also affect the stress development. The CCFST truss (T2) is selected herein to illustrate the stress and strain developments when typical moments are reached based on the FEA modelling. Since the local joint failure does not occur in the FEA simulation, point D is simply defined as the moment when the same deflection as that of the specimen T1-1 at peak load is reached.

The typical longitudinal stress development of concrete at mid-span section is shown in Fig. 7. The trend of the stress distribution remains the same during the whole loading process, with the bottom chord in tension and top chord in compression. When the steel tube of the bottom chord yields at point A, the infill concrete in the bottom chord has already cracked and the maximum tensile stress is 3.97 MPa which is smaller than the tensile strength (4.62 MPa). The tensile stress decreases further as the loading continues.

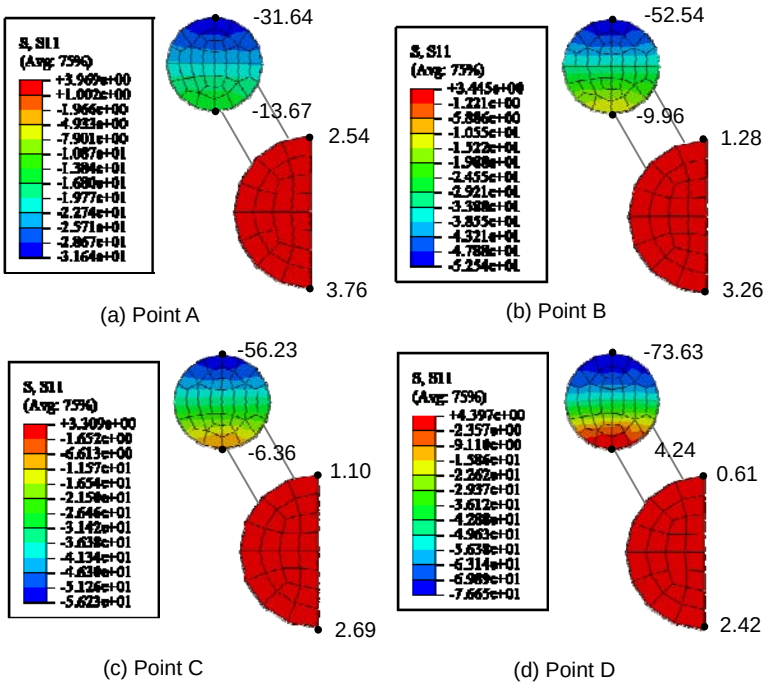

Fig. 7 Typical stress distribution of the CCFST truss at mid-span section (Unit: MPa)

In terms of the concrete in the top chord, the longitudinal stress at the upmost point of the cross section keeps increasing during the loading process. At point D, the maximum compressive stress reaches 76.65MPa ($1.28f_c'$) resulting from the confinement by the steel tube. But the stress at the bottommost point is always much smaller, indicating that the top chord is subjected to combined compression and bending. At Points C and D, the concrete at the bottom of the cross section is subjected to tension rather than compression due to the stress redistribution. The neutral axis also moves up gradually from a location between the two chords to a location inside the top chord.

The longitudinal plastic strain developments of the steel and concrete of the CCFST truss are shown in Figs. 8 and 9, respectively. Due to the low tensile strength of concrete, plastic strain develops first in the concrete of the bottom chord at point A, whilst the steel is almost in the elastic stage. As the load increases, the plastic strain develops at the bottom chord of the middle span in both the concrete and steel components of the CCFST truss until point D. On the other hand, the braces and the parts of the chords near the support are relatively safe with nearly no plastic strain developed during the loading process. At point D, the maximum plastic strains of both the concrete and steel reach about 0.02, which are not large enough to cause tensile failure of the steel but will cause significant cracking of the concrete.

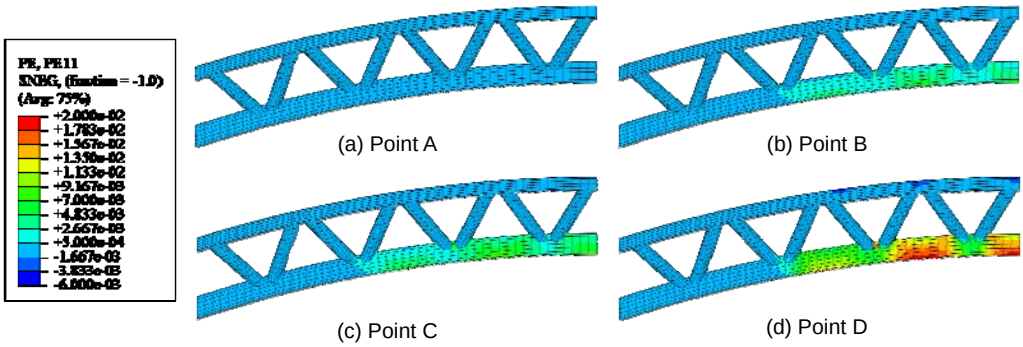

Fig. 8 Typical plastic strain distribution of the steel

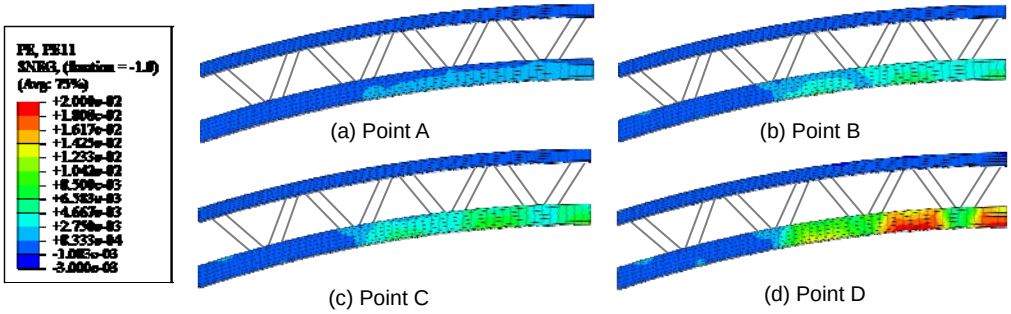

Fig. 9 Typical plastic strain distribution of the concrete

5. Conclusions

The following conclusions can be drawn based on the limited experimental and numerical study reported in this paper:

(1) A finite element analysis (FEA) model of the CCFST truss subjected to bending was developed using ABAQUS. A set of tests is used to verify the FEA model, where good agreement is achieved in predicting the failure modes, load versus deflection curves and load versus strain curves.

(2) A typical load versus deflection curve of CCFST trusses can be divided into three parts: elastic stage, yielding stage and hardening stage. Within the parametric limit of the tested specimens, the bottom tube yields first before the top tube, while the top tube yields before the strain of the bottom tube reaches 10000 $\mu\varepsilon$ which corresponds to the ultimate load.

(3) Full range analysis is conducted to further investigate the mechanical behaviour of the truss. The results show that stress redistribution occurs because of the plasticity of materials. Due to the excellent performance of CFST chords in compression, the top chord is much stronger than the bottom chord, which leads to large plastic deformation in the bottom chord.

Acknowledgements

The research reported in the paper is part of Project 50978150 supported by National Natural Science Foundation of China, as well as Tsinghua University Initiative Scientific Research Program (No. 2011THZ03). The financial support is highly appreciated. The Authors also wish to thank Dr. Ren Qinxin and Dr. He Shanhu for their assistance in the tests.

References

Fong, M., Chan, S.L. and Uy, B. (2011), "Advanced design for trusses of steel and concrete-filled tubular sections", *Eng. Struct.*, **33**(12), 3162-71.

Han, L.H. (2004), "Flexural behavior of concrete-filled steel tubes", *J. Constr. Steel Res*., **60**(2), 313-37.

Han, L.H., He, S.H., Zheng, L.Q. and Tao, Z. (2012), "Curved concrete filled steel tubular (CCFST) built-up members under axial compression: Experiments", *J. Constr. Steel Res*., **74**, 63-75.

Han, L.H., Yao, G.H. and Tao, Z. (2007), "Performance of concrete-filled thin-walled steel tubes under pure torsion", *Thin-Walled Struct.*, **45**(1), 23–6.

Han, L.H., Zheng, L.Q., He, S.H. and Tao, Z. (2011), "Tests on curved concrete filled steel tubular members subjected to axial compression", *J. Constr. Steel Res*., **67**(6), 965-76.

Hibbitt, Karlson and Sorensen (2004), ABAQUS Version 6.5: theory manual, users' manual, verification manual and example problems manual, HKS Company, America.

Jin, M., Zhao, J.C., Liu, M.L. and Chang, J. (2011), "Parametric analysis of mechanical behavior of steel planar tubular truss under fire", *J. Constr. Steel Res*., **67**(1), 75-83.

Kawano, A. and Matsui, C. (2000), "The deformation capacity of trusses with concrete filled tubular chords", *Proceeding of the Composite Construction in Steel and Concrete **IV***, 734-45.

Kawano, A. and Sakino, K. (2003), "Seismic resistance of CFT trusses", *Eng. Struct.*, 2003, **25**(5), 607-19.

Lu, H., Han, L.H. and Zhao, X.L. (2009), "Analytical behavior of circular concrete-filled thin-walled steel tubes subjected to bending", *Thin-Walled Struct.*, **47**(3), 346-58.

Rahami, H., Kaveh, A. and Gholipour, Y. (2008), "Sizing, geometry and topology optimization of trusses via force method and genetic algorithm", *Eng. Struct.*, **30**(9), 2360-9.

Tao, Z., Uy, B., Liao, F.Y. and Han, L.H. (2011), "Nonlinear analysis of concrete-filled square stainless steel stub columns under axial compression", *J. Constr. Steel Res*., **67**(11), 1719-32.

Varma, A.H., Ricles, J.M., Sause, R. and Lu, L.W. (2002), "Seismic behavior and modeling of high-strength composite-filled steel tube (CFT) beam-columns", *J. Constr. Steel Res*., **58**(5-8), 725-58.

Wardenier, J., Kurobane, Y., Packer, J.A., Vegte, G.T. and Zhao, X.L. (2008), Design guide for circular hollow section (CHS) joints under predominantly static loading, 2nd Edition, CIDECT Series "Construction with hollow steel sections" No.1, CIDECT.